Review

Diagnostic imaging in infectious keratitis: a review

Maria Cabrera-Aguas * and Stephanie L Watson

Posted Date: 21 August 2023

doi: 10.20944/preprints202308.1468.v1

Keywords: infectious keratitis, corneal imaging, in vivo confocal microscopy, optical coherence tomography, artificial intelligence, deep learning, microbial keratitis

Review

Diagnostic Imaging in Infectious Keratitis: A Review

Maria Cabrera-Aguas [1,2] and Stephanie L. Watson [1,2]

[1] The University of Sydney, Save Sight Institute, Discipline of Ophthalmology, Faculty of Medicine and Health, Sydney, New South Wales, Australia
[2] Sydney Eye Hospital, Sydney, Australia
* Correspondence: **author:** Dr Maria Cabrera-Aguas The University of Sydney, Save Sight Institute, Sydney Eye Hospital, South block, Level 1, 8 Macquarie St, Sydney NSW 2000, T: +61 2 9382 7287, M: +61 431 737 428 E: maria.cabreraaguas@sydney.edu.au

Abstract: Infectious keratitis (IK) is among the top 5 leading causes of blindness globally. Early diagnosis is key to guide an appropriate therapy to avoid complications such as vision impairment and blindness. Culture of corneal scrapes is the initial diagnostic test to grow and identify the causal organism. Alternative diagnostic tools include imaging such as with optical coherence tomography (OCT) and in vivo confocal microscopy (IVCM). OCT's advantage is its ability to accurately determine the depth and extent of the corneal ulceration, infiltrates and haze; therefore, characterizing the severity and progression of the infection. However, it is not a preferred choice in the diagnostic tool package for infectious keratitis. IVCM is a great aid in the diagnosis of fungal and Acanthamoeba keratitis with overall sensitivities of 66-74% and 80-100%, and specificity of 78-100% and 84-100%, respectively. Recently the use of deep learning (DL) models in IK has been shown to aid diagnosis via image recognition. Most of the studies that have developed DL models to diagnose the different types of IK have utilised photographs from digital camaras, slit-lamp images, or IVCM images. Some studies have used extremely efficient single DL algorithms to train their models and others used ensemble approaches. This technology is likely to assist in the diagnosis of IK in some years. Further work is needed to examine and validate the clinical performance of the DL models in the real-world setting and to evaluate whether this technology improves patient clinical outcomes. The scope of this review was to provide a recent update on the diagnostic imaging tools in IK.

Keywords: infectious keratitis; corneal imaging; in vivo confocal microscopy; optical coherence tomography; artificial intelligence; deep learning; microbial keratitis

1. Introduction

The cornea is essential for vision and contributes 3/4th of the eye's refractive power. While cataracts in the developing world, and age-related macular degeneration (in the older patients) in the developed world, are recognised as the leading causes of visual impairment; corneal blindness affects all ages, and is a leading cause of irreversible visual impairment [1]. Despite continuous efforts to combat this disease, infectious corneal ulceration (infectious keratitis) still receives insufficient global attention [1]. Corneal ulceration (opacity) is among the top 5 causes of blindness and vision impairment globally [1–3]. The most recent data in 2020 reported that 2.096 million people older than 40 years of age are blind and 3.372 million people have moderate to severe vision impairment from non-trachomatous corneal opacity.[2]

Infectious keratitis is an ophthalmic emergency requiring immediate attention as it can progress rapidly to loss of the eye in some cases [4]. A diagnosis of infectious keratitis is made from the patient's history, clinical examination under the slit-lamp and the microbiology results from staining and culture of the scrapings from the corneal ulcer [4,5]. The key to making the diagnosis is the identification of an epithelial defect by slit-lamp examination with fluorescein staining [6,7] (Figure 1). Corneal infiltration by leukocytes may also be present but is dependent on the patient's immune response and may be absent in the immunocompromised patient [8] and in patients already on topical steroids. Along with aiding with diagnosis, slit lamp biomicroscopy is used in determining severity of the infection [8]. The indices used for determining severity include the maximum length

 doi:10.20944/preprints202308.1468.v1

and width of the epithelial defect and adjacent infiltrates, the maximal stromal thinning (percentage of normal corneal thickness), the height of the hypopyon if present, and the extent of the anterior chamber inflammation including the amount of any fibrin deposition [8]. In the case of bacterial keratitis, the severity can be classified as mild, moderate and severe. Mild corneal ulcers are those <2mm in size with the depth of the ulcer <20% or with 100 um corneal thickness. Superficial infiltrates near the ulcer may also be seen. Moderate corneal ulcers range between 2 to 5mm in size, depth of 20-50% (100-275 um) of the cornea, with dense infiltrates extending to the mid stroma. Severe ulcers are ≥5mm, with a depth of more than 50% (>275um) and have dense infiltrates reaching the deep layers of the corneal stroma [4,9]. Poor patient outcomes have been associated with increased severity [10].

Figure 1. Corneal ulceration in bacterial keratitis. Note there is an epithelial defect overlying the corneal infiltrate.

Culture of the corneal scraping is the gold standard for diagnosis and to identify and isolate the causal organism of the infection [4,5,11]. However, the positive rate of such cultures ranges between 38-66% [4]. Antimicrobial resistance testing is routinely performed on bacterial isolates with the results typically available after 48 hours. Empiric antimicrobial therapy is commenced whilst awaiting these results to avoid a serious complication such as loss of vision or even loss of the eye [4]. Due to the limitations of corneal scraping in recent years, a range of imaging techniques have been used to aid the diagnosis of and severity grading of infectious keratitis. Understanding the current state of advances in corneal imaging for keratitis will be of benefit to clinicians in practice and researchers interested in the field. The aim of this review was to describe the current corneal imaging diagnostic tests used in infectious keratitis.

2. Optical coherence tomography

In 1994 it was shown that the anterior chamber could be imaged using optical coherence tomography (OCT) with the same frequency of 830 nm used in posterior chamber imaging [7,12]. This advance has enabled imaging and analysis of structures such as the cornea and the anterior chamber angle. The predominant market for OCT applications has been for retinal imaging. The first commercial anterior segment devices, known as anterior segment optical coherence tomography (AS-OCT), that became commercially available were modified posterior chamber devices. Some of these AS-OCT devices were stand alone, and others required modifications, such as an additional lens to modify the posterior chamber OCT devices. Modifications in 2001, to the light source and lens of the

Preprints (www.preprints.org) | NOT PEER-REVIEWED | Posted: 21 August 2023 doi:10.20944/preprints202308.1468.v1

AS-OCT, enabled higher frequency waves (1310nm) to allow a higher resolution of the image and more precise measurement [7,13].

AS-OCT is now a well-recognized method for imaging the cornea and is often used in anterior chamber angle imaging for glaucoma [7,11]. The AS-OCT advantage over the slit-lamp is its ability to accurately determine and delineate the depth and extent of the corneal ulceration, infiltrates and haze to characterise, quantify and monitor the progress of corneal pathologies such as superficial and deep infectious keratitis [11]. Other applications of the AS-OCT include measurement of corneal thickness to determine the risk of corneal perforation; prediction of the treatment response of infectious keratitis following therapeutic corneal cross-linking (PACK-CXL) and highlighting corneal interface pathologies such as interface infectious keratitis following lamellar keratoplasty (hyper-reflective band at the graft-host interface) [14] or post-LASIK epithelial ingrowth (flap-host interface) [15] and valvular and direct non-traumatic corneal perforations associated with infectious keratitis [11,16]. With the increasing popularity of Small Incision Lenticule Extraction (SMILE) as a refractive procedure, AS-OCT will have a role in identifying and defining interface infections. [17,18] Intra-operative OCT is also emerging as a useful tool and may have applications in surgery for infectious keratitis but enabling delineation of involved structures. (Figure 2)

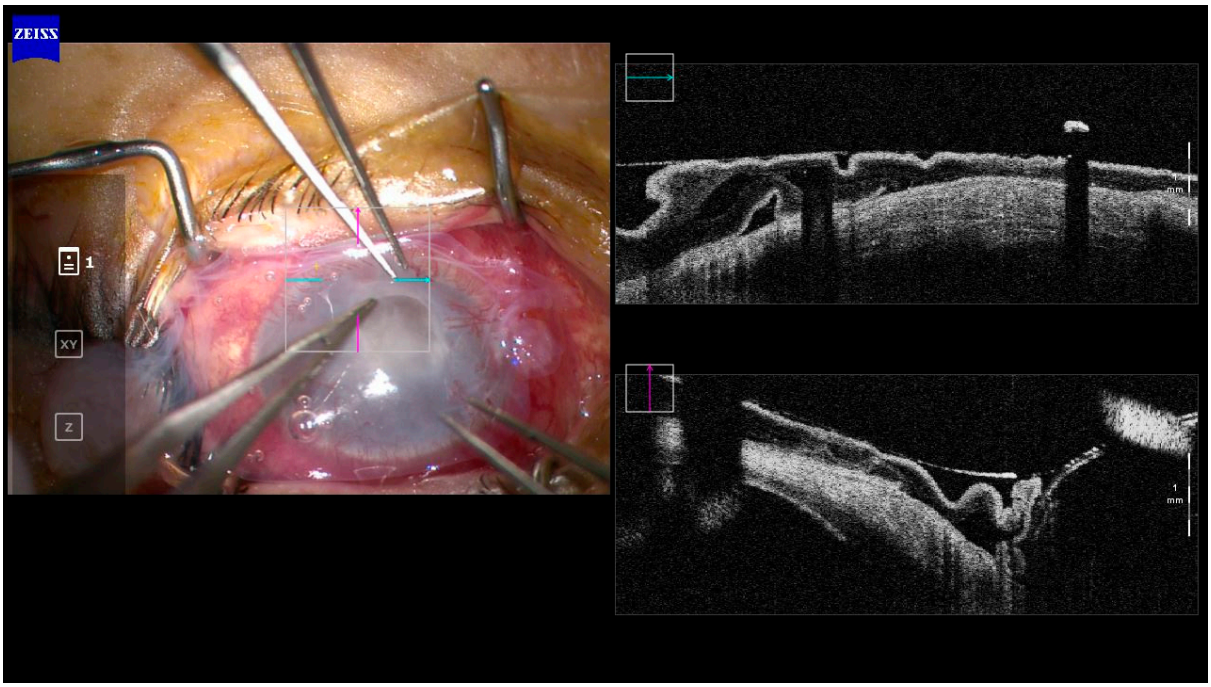

Figure 2. Intra-operative OCT in a case of amniotic membrane transplant for a persistent epithelial defect post-microbial keratitis.

2.1. Types of AS-OCT

Optical coherence devices in current clinical use can be classified according to the type of image sampling as Time domain, Spectral Domain, and Swept Source. Each class of OCT has different a sampling method depending on the sampling speed and resolution, and with each change there are implications for the application of AS-OCT.

2.1.1. Time Domain OCT

Time Domain (TD) OCT was the first generation to be used in clinical practice [19]. The TD-OCT directs a near Infrared (IR) light at the retina and encodes the location of the back-reflected light based on time of flight by relating the reflection location to the position of a moving reference mirror [19]. The two models available were the SL-OCT (Heidelberg Engineering) and the Visante (Carl Zeiss Meditec, Inc.). The Spectralis AS – OCT (Heidelberg) is a lens module that is attached to a posterior

 doi:10.20944/preprints202308.1468.v1

chamber OCT. The Visante (Carl Zeiss) is a stand-alone unit for anterior segment imaging [7]. Both of these devices were only able to generate 400 axial scans per second due to limitations of the moving mirror components. In addition to the limitations in scanning speed, these devices also had limited resolution (both axial and transverse) [7,19].

The use of TD- OCT for imaging the cornea in infectious keratitis has been investigated in two studies; a cross-sectional observational study of 26 eyes by Konstantopoulos et al., and a case series of two eyes by Abbouda et al. [7,12,20]. Konstantopoulos et al. reported that parameters indicating the progression of infectious keratitis, such as corneal and infiltrate thickness at the centre of the lesion, were able to be calculated in a reliable and accurate method using TD OCT (Visante OCT; Carl Zeiss Meditec Inc, Dublin, CA). This cross-sectional study also found that TD OCT could differentiate *Pseudomonas aeruginosa* keratitis from other forms of keratitis due to the larger width of the lesion ($p=0.003$), corneal thickness ($p= 0.001$), and infiltrate thickness ($p = 0.057$) at initial presentation, and a more rapid reduction of corneal thickness in the first few days [7,12]. Their findings agreed with the acute and intense inflammatory response seen in animal models of *P. aeruginosa* keratitis [7,21]. Abbouda et al., reported in a case series of two eyes, that TD OCT could be used to guide corneal crosslinking treatment in severe infectious keratitis by indicating the depth of the infiltrate and degree of inflammation. But found that the limited resolution of TD OCT contributed to its inability to differentiate scars from infiltrates [7,12,20]. This limitation of TD OCT compromised its ability to determine whether there was an active infectious keratitis.

2.1.2. Spectral Domain OCT

Spectral-domain (SD) OCT evaluates the frequency spectrum of the interference between a stationary reference mirror and the reflected light, allowing spatial and structural information to be measured simultaneously at all echo time delays (axial pixels). The benefit of simultaneous assessment of all axial-depth scan (A-scan) pixels is the significant increase in scanning speed up to 100,000 A-scans/s with commercial devices and up to 20.8 million A-scans/s with research devices [19]. In addition, a higher resolution, up to 2 microns, was achieved via a broader spectrum light source [7,22]. SD-OCT has been used to assess corneal pathology such as scarring and thinning (Figure 3A) and measure corneal thickness and show epithelial layer thickness (Figure 3B).

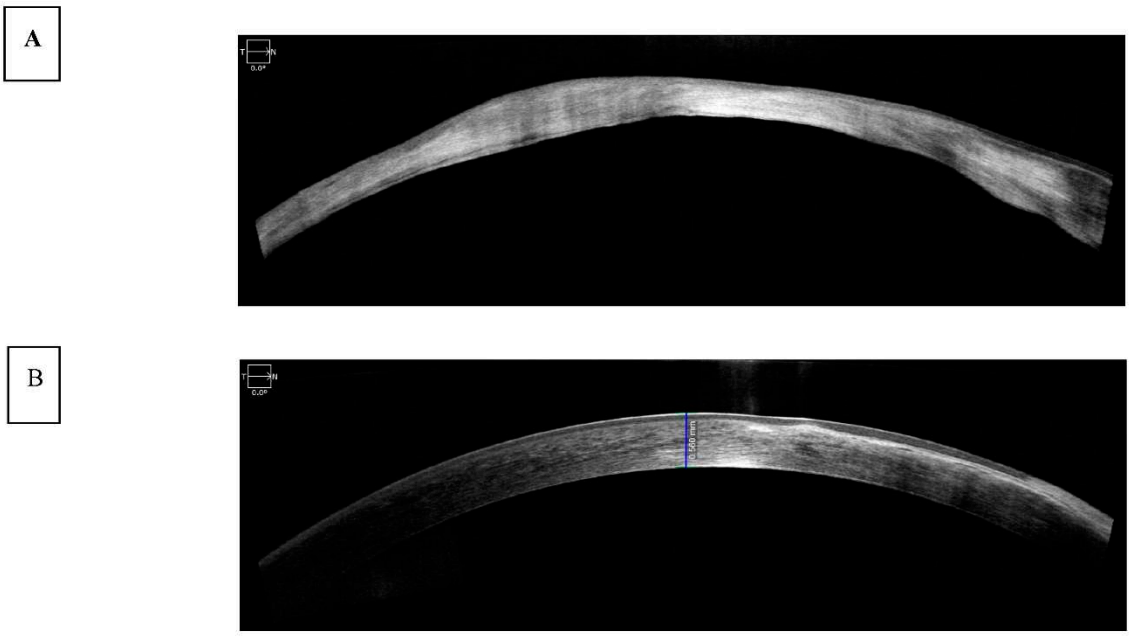

Figure 3. A and 3B: SD-OCT images of the cornea showing A) Corneal scarring and thinning in a patient following acanthamoeba keratitis and B) corneal thickness measurement and epithelial layer imaging.

 doi:10.20944/preprints202308.1468.v1

The use of spectral domain (SD) OCT in infectious keratitis has been reported in one cross-sectional study of 22 eyes by Soliman et al. [23], one case series with 4 eyes by Yamazaki et al. [7,24] and one cross-sectional study of 25 patients by Oliveira et al. [25]. Using SD OCT (RTVue-100; Optovue, Freemont, CA, USA), Soliman et al., was able to distinguish infiltrates form scars, potentially allowing for the distinction of different stages of infectious keratitis as well as potentially identifying non-infective causes [7,11,23]. They found that although both infiltrates and scars were hyper-reflective, corneal infiltrates (Figure 1) had overlying defects or 'opaque epithelial layers', in combination with poorly defined and rounder borders. In contrast, scars had well defined edges with a defect-free epithelium. In addition, cystic spaces were identified in some active lesions which could be correlated to areas of necrosis. By combining this classification with the layer of the cornea that the lesion occurred in, and the presence of fluorescein (as seen on slit-lamp analysis), the group generated 12 distinct characteristics. The characteristics were grouped by the causal microbes to try and identify any further patterns. For example, the localized small stromal cystic spaces interpreted as localized stromal necrosis and full thickness large stromal cystic spaces as diffuse stromal necrosis were found to be only associated with fungal infections due to Aspergillus species. On the other hand, the diffuse stromal thinning with an epithelial defect on top with thin positive fluorescein staining was only found with *Staphylococcus aureus* infections. Such that spectral domain OCT has the potential to assist the identification of the causal microbe in cases of IK. This study was limited due to a small sample size such that a larger study is needed to determine the sensitivity and specificity for each type of keratitis [7,23].

In a case series of 4 eyes, Yamazaki et al. proposed that SD OCT (Spectralis AS – OCT; Heidelberg, Germany) could be used to identify Acanthamoeba in vivo using corneal imaging [7,24]. This was done by correlating highly reflective bands or oblique lines in the corneal stroma with the areas that corresponded to the infiltrate from an established confocal microscopy method, as well as to slit lamp images. This demonstrated a unique OCT pattern for Acanthamoeba that needs to be validated on a larger scale in future studies [7,24].

2.1.3. Swept Source

Swept-source OCT (SS-OCT) scans at faster speeds of up to 200,000 A-scans/s with current commercial devices and millions of A-scans/s with laboratory devices. This type of tomography uses a laser that quickly sweeps through frequencies across a broad-spectrum contrary to SD-OCT which uses a broad-bandwidth light source [19,26]. SS-OCT permits high scan speeds (shorter scan speeds and higher scan density), less depth-dependent signal-to- noise ratio and resolution drop-off, and improved scan quality (less eye movement). Most SS-OCT devices also use a centre wavelength of approximately 1,050 nm (SD-OCT uses a centre wavelength of approximately 850 nm), which allows for greater axial depth imaging and permits better visualization of deeper ophthalmologic structures such as the choroid and the lamina cribrosa (LC) [19,27,28].

A prospective study with 68 patients aimed to demonstrate a link between the latest OCT technology and clinical outcomes by using a severity index scoring tool. Corneal structures were evaluated by analysis of OCT images of patients with infectious keratitis on the day of presentation and after 6 days. Clinical signs of the infection such as corneal thickness, corneal infiltrates, corneal ulceration, and epithelial defects on the cornea were identified and assessed (Figure 4). These characteristics were used to generate a severity score based on a point system (Table 1). Features of infectious keratitis were identified on OCT analysis in all cases on day zero, and 48 (71%) cases on day six (Figure 5). The most frequent findings were epithelial defect (100%) and stromal oedema noted as corneal thickening. There were corneal thickness changes in 57 (84%) cases on day zero, with 25 (37%) of these having a change between 5-10%, 18 (32%) having a change between 10-30%, 9 (16%) having a change 30-50%, and 5 (9%) having a change >50%. On day zero, there was corneal thickness changes in 89% of *Pseudomonas aeruginosa*, 26% of *Staphylococcus* spp. and 100% of *Streptococcus pneumoniae* cases. [7]

Preprints (www.preprints.org) | NOT PEER-REVIEWED | Posted: 21 August 2023 doi:10.20944/preprints202308.1468.v1

Table 1. Point system of the characteristics assessed using AS-OCT in cases of infectious keratitis [7].

Characteristic on AS-OCT	Points
Corneal thickness change 5-10%	1
Corneal thickness change 10-30%	2
Corneal thickness change 30-50%	3
Corneal thickness change >50%	4
Epithelial defect 0.1-1 x 0.1-1	1
Epithelial defect 1-2 x 1-2	2
Epithelial defect 2-3 x 2-3	3
Epithelial defect >3->3	4
Hypopyon	1
Infiltrates 0.1mm - 1	1
Infiltrates >1	2
Stromal thinning	1
Cysts	1
Scarring	1
Fibrin deposits	1
Total	28

Key: AS-OCT= anterior segment optical coherence tomography.

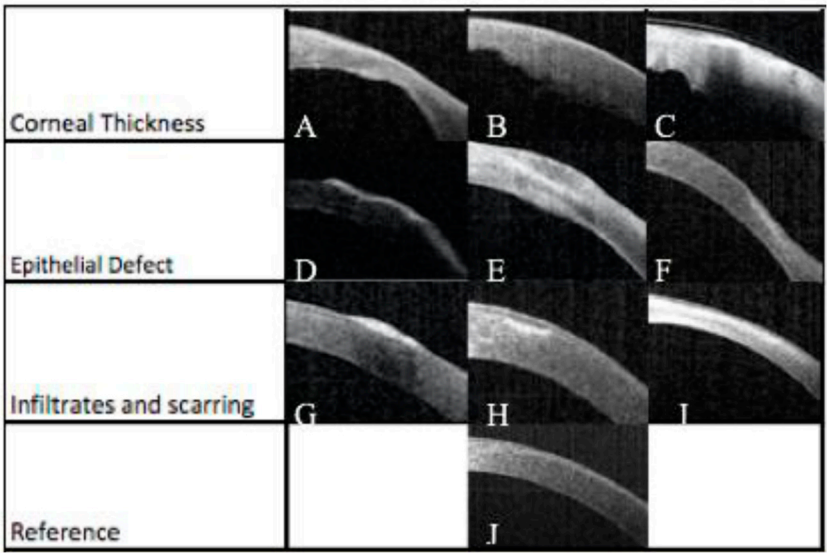

Figure 4. AS-OCT images demonstrating the characteristics of infections keratitis A) Corneal thinning 30-50% with stromal oedema and epithelial defect B) Corneal Thinning 5-10% with stromal oedema C) Stromal thinning 30-50% and stromal oedema D) Long epithelial defect with underlying hypereflective region, that would progress to Descemetocele E) Epithelial defect with underlying scarring F) Epithelial defect with infiltrate G) Epithelial defect with infiltrate and hyporeflective region H) hyperreflective infiltrate I) Corneal thinning with scarring J) example of reference in unaffected eye. [7].

Preprints (www.preprints.org) | NOT PEER-REVIEWED | Posted: 21 August 2023 doi:10.20944/preprints202308.1468.v1

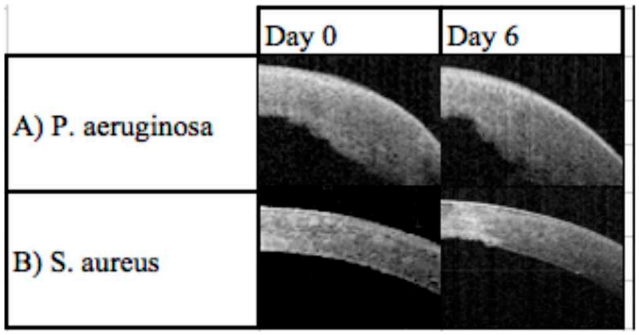

Figure 5. Example of serial features. A) Pseudomonas aeruginosa on day zero and day six with oedema, epithelial defect and poor progression. The outcome in this case was surgery. B) Staphylococcus aureus at day zero and day 6 with infiltrates and scar [7].

In this study, 12 patients required tarsorrhaphy or corneal gluing; six patients, deep anterior lamellar keratoplasty (DALK), and one vitrectomy. The average score of the surgical patients was 19. The patients who required surgery had a significantly higher score than those that reached resolution without intervention (p= 0.042). There was no statistical association between a single feature on AS-OCT and a surgical outcome. There was a significant correlation between patients whose scores on day six were the same or higher than day zero and the requirement of surgery (p= 0.003). Patients with improvement in severity score from day zero to day six were more likely to not require surgery (p=0.027). This study demonstrated that characteristics evident on AS-OCT analysis correlated with clinical outcome and the need for surgical intervention. [7] Further work is needed to validate these findings for clinical use.

3. In vivo Confocal microscopy

Another non-invasive imaging tool is in vivo confocal microscopy (IVCM) which provides a high-resolution, in vivo assessment of corneal structures and pathologies at a cellular and subcellular level [11]. IVCM provides corneal images with a resolution of 1 μm, from the epithelium to endothelium, nerves and cells, sufficient to yield images larger than a few micrometres of filamentous fungi or Acanthamoeaba cysts [4,29–31]. A third-generation laser scanning confocal microscope Heidelberg Retinal Tomograph (HRT3) in conjunction with the Rostock Cornea Module (RCM) (Heidelberg Engineering, Germany) uses 670 nm red wavelength and high-resolution images with lateral resolution close to 1 μm, axial resolution of 7.6 μm and 400x magnification. This has improved the sensitivity of this technique allowing the identification of yeasts, which could not be reported previously with the first-generation confocal microscopes [11,30–33].

IVCM had been mainly used in the evaluation of fungal and Acanthamoeba keratitis (AK) due to its axial limitation of 5-7 μm which is not sufficient to detect bacteria (less than 5 μm) and virus (in nanometres) [4,11,33]. IVCM has been a great ally to the microbiological diagnostic tests as it can identify these organisms rapidly overcoming the tests variable positive rate of between 40-99% and a turnaround time of up to 2 weeks [11]. Therefore, an imaging diagnostic test is valuable to guide initial therapy.

Sensitivity of IVCM in fungal keratitis has been reported as between 66.7% and 94%, and specificity between 78% and 100% [4,30,33–36]. Filamentous fungal keratitis is predominately caused by *Aspergillus spp.* and *Fusarium spp*. [4,33]. Aspergillus spp. are 5-10 μm in diameter and have septate hyphae with dichotomous branches at a 45-degree angle. On the other hand, *Fusarium* spp. typically branches at 90-degree angle. Hyper-reflective elements must be differentiated from the basal corneal epithelial nerves which have more regular branching, whereas stromal nerves are much large in diameter (25-50 μm) and *Aspergillus spp.* and *Fusarium* spp. are 200-400 μm long [11,33]. Yeast-like fungi (*Candida spp*.) can also cause keratitis with a predilection for the immunosuppressed (Figure 6); they appear as elongated, hyper-reflective particles resembling pseudohyphae of 10-40 μm in length and 5-10 μm in width [11,33].

 doi:10.20944/preprints202308.1468.v1

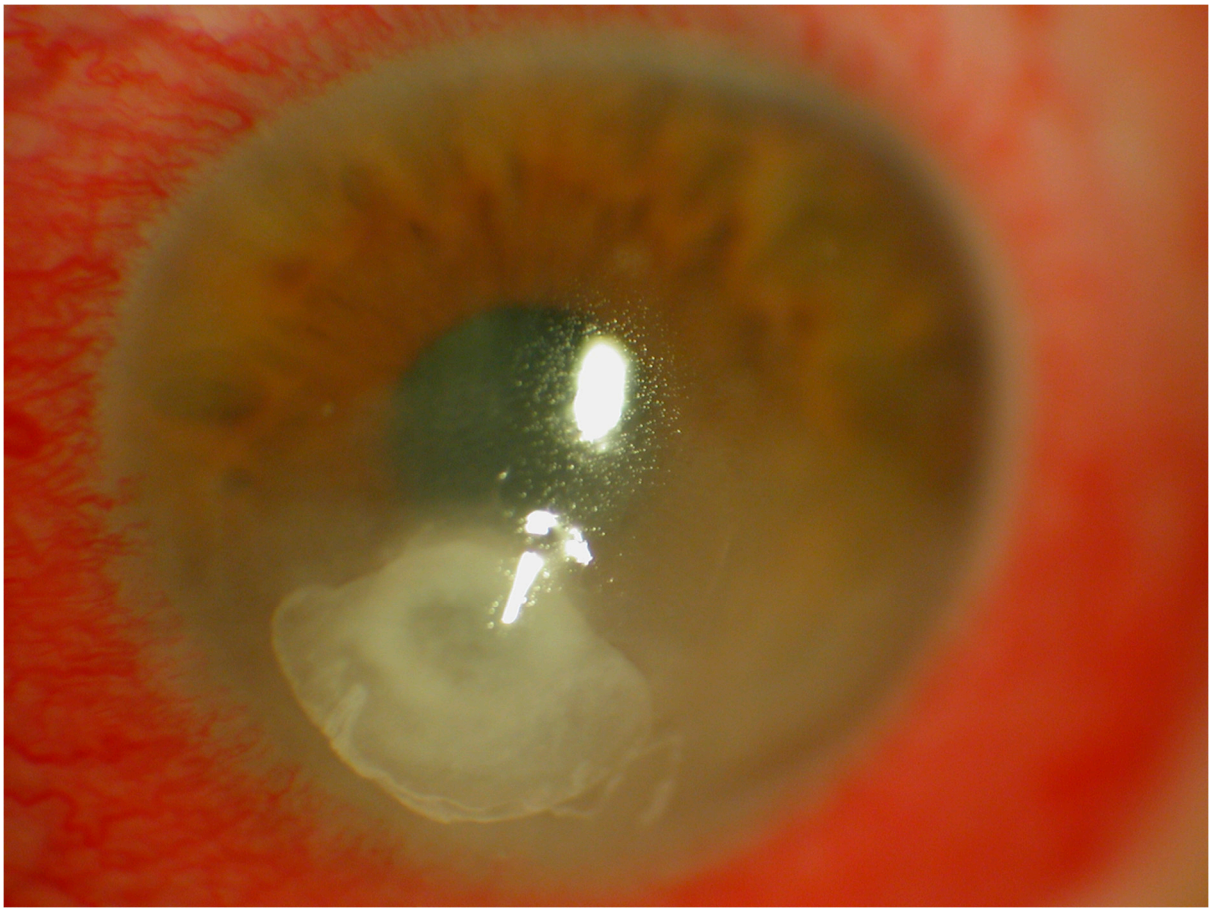

Figure 6. Candida albicans keratitis in a patient on immunosuppression.

IVCM is a key diagnostic test in AK with an overall sensitivity of 80-100% and specificity of 84-100% [11,34–38] A*canthamoeba spp.* can present as cysts or trophozoites. Cysts (dormant form) appear as hyperreflective, spherical and well-defined double-wall structures of ~ 15-30 μm in diameter in the epithelium or stroma. Trophozoites (active form) appear as hyper-reflective structures of 25-40 μm which are difficult to discriminate from leukocytes and keratocyte nuclei. [4,11,39]. *Acanthamoeba spp*. can also present as bright spots, signet rings and perineural infiltrates. Perineural infiltrates are a pathognomonic characteristic of AK which appears a reflective patchy lesions with surrounding hyper-reflective soindle-shaped materials [11] (Figure 7).

Preprints (www.preprints.org) | NOT PEER-REVIEWED | Posted: 21 August 2023 doi:10.20944/preprints202308.1468.v1

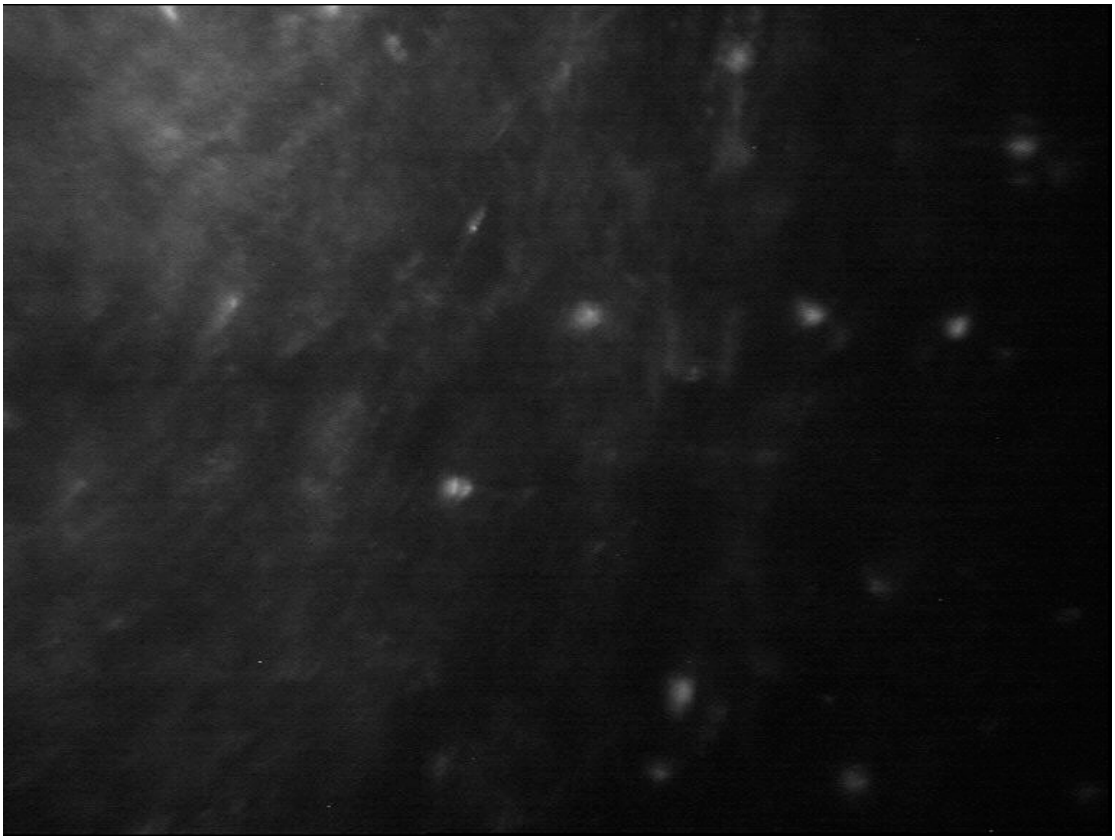

Figure 7. In vivo confocal microscopy of Acanthamoeba keratitis.

Advantages of IVCM include 'non-invasiveness', rapid, real-time and early identification of the organism, for monitoring and guidance of the therapy, and determination of the depth of the infection. Early identification and treatment of AK has been associated with improved prognosis [4,40]. It also allows the possibility of longitudinal exams in the same patient which may be of use in determining resolution and provides quantitative analysis of all cornea layers, nerves and cells to assess severity. Limitations of IVCM include the need for an experienced operator, patient co-operation, unsuitability for smaller organisms, motion artefacts, cost of the device and dense corneal infiltrates and/or scarring can affect the proper tissue penetration and visualization [4,29–31,33]

In clinical practice, typically, IVCM is performed in cases of progressive keratitis, suspicion of AK or FK, negative culture result, deep infection due to natural clinical course or fungal keratitis or development of interface infectious keratitis following corneal surgeries which limits access of conventional microbiological tests [4,11].

4. Artificial intelligence - Deep learning methods

The applications of artificial intelligence in health care are now a reality due to the advancement of computational power, refinement of learning algorithms and architectures, availability of big data and easy accessibility to deep neural networks by the public [41–43]. Deep learning algorithm mostly uses multimedia data (images, videos and sounds) and involves the application of large-scale neural networks such as artificial neural network (ANN), convolutional neural network (CNN) and recurrent neural network (RNN) [42]. The advantage of deep CNNs is learning the feature representation from data without human knowledge and the capability of processing large training data with high dimensionality [44]. A CNN model contains multiple convolutional layers, pooling layers and activation units which is trained using model images by minimizing a pre-defined loss function. A convolutional layer applies a number of filters to the input image calculated from the previous layer. This results in enhanced features at certain locations in the image. The weights in these filters are learned during the training process. A pooling layer is a dimensionality reduction

Preprints (www.preprints.org) | NOT PEER-REVIEWED | Posted: 21 August 2023 doi:10.20944/preprints202308.1468.v1

operator that down-samples the input image obtained from the previous layer. Average and max are the most popular pooling operators, which calculate the average and max value of a local region during the image down-sampling process, respectively [44].

Some common terminologies used in AI studies are showed in Table 2A and 2B [44]. The sensitivity (Y-axis) and specificity (X-axis) rates are used to illustrate the receiver operating characteristic (ROC) curve and the area under the ROC curve (AUC) which are used to determine the performance of a model at all thresholds. An AUC of 1 is a 'perfect' classifier, AUC between 0.5-1 is a real-world classifier and AUC of 0.5 is a 'poor' classifier which is not better than a random guess [44].

Table 2. A: Definitions of common terminologies in disease screening [44].

		Actual outcome	
		Disease	No Disease
Predicted outcome	Disease	TP	FP
	No Disease	FN	TN

Table 2. B: Definitions of common terminologies in artificial intelligence studies [44].

Sensitivity	**TP/(TP+FN)**	**Actual positive cases predicted correctly by model**
Specificity	TN/(TN+FP)	Actual negative cases predicted correctly by model
PPV (Precision)	TP/(TP+FP)	Positively classified cases that were actually positive
NPV	TN/(TN+FN)	Negatively classified cases that were actually negative
Accuracy	(TP+TN)/(TP+TN+FP+FN)	Overall accuracy in predicting both positive and negative cases.

TP = True positive; FP = False positive; FN = False negative; TN = True negative; PPV = Positive predictive value; NPV = Negative predictive value.

The DL CNN model training needs to consider several aspects. The quality of the training dataset is essential to the performance of the DL CNN model. Clinicians usually provide the image annotation including pixel-level annotation or image-level annotation or both. The model may suffer from over-fitting that cannot be generalized well to new test data due to many model parameters and relatively small training examples. A validation dataset is generally used to determine the training termination point for avoiding model over-fitting. Drop-out, data augmentation, and transfer learning have been used to improve the generalizability of a trained model. An independent external test set is used to evaluate the trained ML model for assessing the generalizability of the method. A lower performance normally occurs when testing on an independent test set, which is mainly due to model overfitting to the training dataset or a data distribution discrepancy between the training and testing datasets. Figure 8 illustrates an example of a CNN training and evaluation framework.

Preprints (www.preprints.org) | NOT PEER-REVIEWED | Posted: 21 August 2023 doi:10.20944/preprints202308.1468.v1

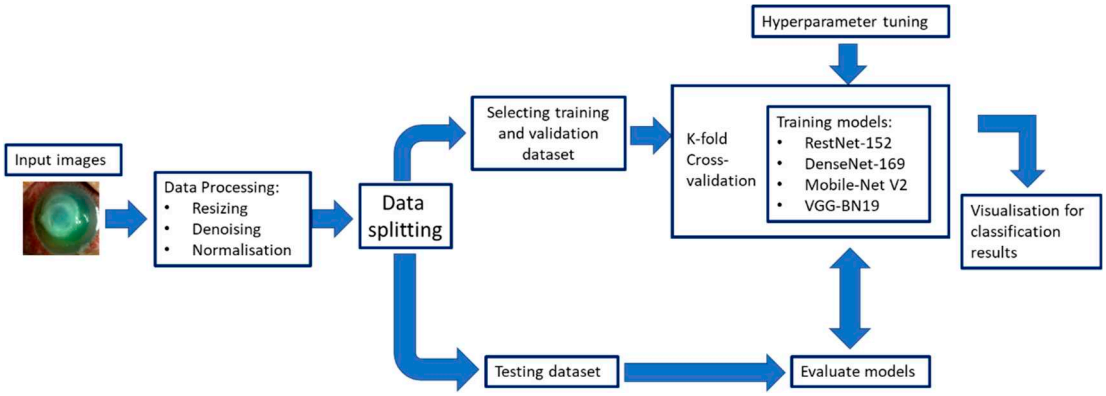

Figure 8. Flow diagram of a convolutional neural network training and evaluation procedure.

In 2016, the use of artificial intelligence (AI) with deep learning (DL) in ophthalmology initially focused on posterior segment diseases such as diabetic retinopathy and age-related macular degeneration; but its application in diseases of the cornea, cataract and anterior chamber structures has surged in the last years [41]. Corneal AI research has focused on diseases that require corneal imaging for determining an appropriate management with slit-lamp photography, corneal topography, and anterior segment optical coherence tomography [41]. For infectious keratitis, the use of DL with CNNs has shown to potentially be a more accessible diagnostic method via image recognition [4,45,46]. Many studies have evaluated DL methods for diagnosing IK using images taken with a handheld camara, camara mounted on a slit-lamp, or confocal microscopy [42,45,47–55]. Several extremely efficient DL algorithms include RestNet-152 [56], DenseNet-169 [57], Mobile-Net V2 [58], and VGG-19_BN [59]. Recent studies have used an ensemble approach which uses many learning algorithms to perform the same classification task yielding better validity and improved generalization performance [52,60]. The CNN-based ensemble approach takes elements of the different CNN algorithms to build the final model. Some studies have reported that the ensemble DL model could better classify the stages of diabetic retinopathy and glaucoma using fundus photos than a single CNN model [52].

Redd et al. used images from handheld cameras to train 5 CNNs to differentiate FK to BK and compare their performance against human experience. The best performing CNN was MobileNet with AUC of 0.86. The CNNs group achieved a statistically significant higher AUC (0.84) than the experts (0.76, $P<0.01$). CNNs elicited higher accuracy for FK (81%) versus BK (75%) compared to the experts who showed more accuracy for BK (88%) versus FK (56%) [45]. Wang et al. investigated the potential of DL in classifying IK using slit-lamp images and smartphone photographs. They also studied whether any information from the sclera, eyelashes and lids could improve the diagnosis of keratitis. The slit-lamp images (global image) were pre-processed excluding the irrelevant background (regional image). For the smartphone photographs, a small patch was extracted so make it look similar to the global slit-lamp image. Three CNNs were assessed. The InceptionV3 showed a better performance with AUC of 0.9588 on global images, 0.9425 on regional images and 0.8529 for smartphone images; while the two ophthalmologists reached an AUC of 0.8050 and 0.7333, respectively. The lower performance of the smartphone images could be caused by multiple factors including the size of the dataset and the significant variation in imaging conditions (*e.g.*, ambient light, camera brand, and focus) [47].

Hung et al. used slit-lamp images to train eight CNNs for identifying BK and FK. The best performing model was DenseNet161 with AUC of 0.85. The diagnostic accuracy for BK ranged from 79.6% to 95.9% and for FK 26.3% to 65.8%, respectively [48]. Kuo et al. aimed to assess the performance of eight CNNs (four EfficientNet and four non-EfficientNet CNNs) in diagnosing BK using slit-lamp images. All non-EfficientNet and EfficientNet models had no significant difference in diagnostic accuracy ranging from 68.8% to 71.7% and AUC from 73.4% to 76.5% [46]. EfficientNet B3 showed the most excellent average AUC with 74% sensitivity and 64% specificity. The diagnostic accuracy of these models (69% to 72%) is comparable to the ophthalmologists (66% to 75%) [46].

Ghosh et al. created the model called DeepKeratitis on top of three pretrained CNNs to classify FK and BK. VVG19 showed highest performance with F1 score of 0.78, precision of 0.88 and sensitivity of 0.70. Applying the ensemble learning model achieved higher performance with F1 score of 0.83, precision of 0.91 and sensitivity of 0.77. F1 score is a harmonic mean of precision and recall. This parameter measures the test performance [53].

Hu et al. proposed a DL system with slit-lamp images to automatically screen and diagnose IK (BK, FK and viral keratitis (VK)). Six CNNs were trained. The EffecientNetV2-M showed the best performance with accuracy of 0.735 and specificity of 0.904, which was also superior to two ophthalmologists. The overall AUC of the EffecientNetV2-M was 0.85 with 1.00 for normal cornea, 0.87 for VK, 0.87 for FK, and 0.64 for BK [61]. Kuo et al. explored eight single and four ensemble DL models to diagnose BK caused by *Pseudomonas aeruginosa.* The EfficientNet B2 model reported the highest accuracy (71.2%) of the eight single-DL models while the best ensemble 4-DL model showed the highest accuracy (72.1%) among the ensemble models. There was no statistical difference in the area under the receiver operating characteristic curve and diagnostic accuracy among these single-DL models and among the four best ensemble models [52]. Natarajan et al. explored the application of three DL algorithms to diagnose herpes simplex virus (HSV) stromal with ulceration keratitis using slit-lamp images. DenseNet had the best performance with 72% accuracy. The AUC was 0.73 with a sensitivity of 69.6% and specificity of 76.5% [54].

Koyama et al. developed a hybrid DL algorithm to determine the causal organism of IK by analysing slit-lamp images. Facial recognition techniques were also used as the faces were recorded from different angles, different levels of lighting and different degrees of resolution. ResNet -50 and InceptionResNetV2 were used. The final model was built based on InceptionResNetV2 using 4306 images consisting of 3994 clinical and 312 web images. This algorithm had a high overall accuracy of diagnosis: AUC for acanthamoeba was 97.9%/0.995, bacteria was 90.7%/0.963, fungi was 95.0%/0.975, and HSV was 92.3%/0.946 [49]. Similarly, Zhang et al. constructed a DL model based on two pre-trained CNNs for early IK diagnosis. KeratitisNet, the combination of ResNext101_32x16d and DenseNet169 had the highest accuracy 77.08%. The accuracy of KeratitisNet for diagnosing BK, FK, AK, and HSK was 70.27%, 77.71%, 83.81%, and 79.31%, and AUC was 0.86, 0.91, 0.96, and 0.98, respectively. KeratitisNet was mostly confused with BK and FK images. 20% of BK cases were mispredicted into FK and 16% of FK cases into BK. The accuracy of the model was significantly higher than an ophthalmologist clinical diagnosis ($p < 0.001$) [50].

Several studies have also investigated the performance of DL CNNs methods in diagnosing FK using IVCM images [41,42]. Wu et al. developed a new automatic hyphae detection method to diagnose FK which has two steps: texture classification of images and hyphae detection. An adaptive robust binary pattern was proposed to extract texture features and a support vector machine models for classifying normal and abnormal images. The accuracy for this classification was of 99.74% [62]. Liu et al. proposed a novel CNN model for automatically diagnosing FK using data augmentation and image fusion. The accuracy of conventional AlexNet and VGGNet were 99.35% and 99.14%. This CNN model perfectly balances diagnostic performance and computational complexity improving real-time performance in diagnosing FK [63]. Lv et al. developed an intelligent system based on the DL CNN (ResNet) model to automatically diagnose FK using IVCM images. The AUC of the system to detect hyphae was 0.9875 with accuracy of 0.9626, sensitivity of 0.9186 and specificity of 0.9834 [64].

5. Limitations

Despite the great advancement of DL with CNNs in the diagnosis of conditions using images; it is still challenging to achieve a satisfactory diagnostic performance in IK. Reasons for this include the large intra-class variance (difficulty in capturing the common characteristics of images in the same class); small inter-class difference (difficulty in discriminating the margin between different classes); poor image quality due to nonstandard protocols increasing the difficulty to find the common special features of the different types of IK; and difficulty in overfitting due to the lack of large scale dataset in IK [55]. To overcome such limitations, Li et al. developed a novel CNN called Class Aware

Attention Network to diagnose IK using slit-lamp images. In this network, a class-aware classification module is first trained to learn class-related discriminative features using separate branches for each class. Next, the learned class-aware discriminative features are fed into the main branch and fused with other feature maps using two attention strategies to assist the final multi-class classification performance [55]. This method showed a higher accuracy (0.70) and specificity (0.89) compared to eight single CNNs. This innovative CNN can extract the fine features of keratitis lesion which are not easy for clinicians to identify [55]. Further there are a wide range of causal organisms in keratitis and varied clinical presentations with regional differences in both [4]. Future studies will be needed to validate the findings of CNN approaches to the diagnosis of IK in a range of global settings.

6. Conclusions

Infectious keratitis is a top 5 leading cause of blindness overall worldwide. Early diagnosis is crucial to guide an adequate management to avoid complications such as vision impairment and blindness. Culture of corneal scrapes is the initial diagnostic test to isolate the causing organism. Alternative diagnostic tools using imaging devices such OCT and IVCM can be also used to track the progression of the infection and to determinate of the causal organism(s). Due to the advancement of deep learning models, many study groups worldwide have been able to develop DL-CNNs models to diagnose the different types of IK using corneal imaging. This technology will probably aid clinicians in accurately diagnose the type of keratitis in the near future. Nevertheless, there are some challenges to overcome to use this technology in health settings including poor image quality, difficulty to find the common special features of the different types of IK, cost, accessibility, and cost-effectiveness. Further work is needed to examine and validate the clinical performance of these CNNs models in the real-world setting with multiethnicity populations and in a variety of global settings to increase the generalisability of the model. Finally, it would be also valuable to evaluate whether this technology assist in improving patient clinical outcomes via prospective clinical trials.

Author Contributions: Conceptualization; methodology; writing-original draft preparation: MCA and SLW; writing-editing: SLW. Both authors have read and agreed to the published version of the manuscript.

Conflicts of interest: The authors declare no conflict of interest.

References

1. Ung L, Acharya NR, Agarwal T, Alfonso EC, Bagga B, Bispo PJ, et al. Infectious corneal ulceration: a proposal for neglected tropical disease status. Bulletin of the World Health Organization. 2019;97(12):854-6.
2. Wang EY, Kong X, Wolle M, Gasquet N, Ssekasanvu J, Mariotti SP, et al. Global Trends in Blindness and Vision Impairment Resulting from Corneal Opacity 1984-2020: A Meta-analysis. Ophthalmology. 2023;130(8):863-71.
3. Flaxman SR, Bourne RRA, Resnikoff S, Ackland P, Braithwaite T, Cicinelli MV, et al. Global causes of blindness and distance vision impairment 1990-2020: a systematic review and meta-analysis. Lancet Glob Health. 2017;5(12):e1221-e34.
4. Cabrera-Aguas M, Khoo P, Watson SL. Infectious keratitis: A review. Clin Exp Ophthalmol. 2022;50(5):543-62.
5. Ngo J, Khoo P, Watson SL. Improving the Efficiency and the Technique of the Corneal Scrape Procedure via an Evidence Based Instructional Video at a Quaternary Referral Eye Hospital. Curr Eye Res. 2020;45(5):529-34.
6. Ting DSJ, Ho CS, Cairns J, Elsahn A, Al-Aqaba M, Boswell T, et al. 12-year analysis of incidence, microbiological profiles and in vitro antimicrobial susceptibility of infectious keratitis: the Nottingham Infectious Keratitis Study. Br J Ophthalmol. 2021;105(3):328-33.
7. Maberly J. Evaluating Severity of Microbial Keratitis Using Optical Coherence Tomography 2021.
8. Allan BD, Dart JK. Strategies for the management of microbial keratitis. Br J Ophthalmol. 1995;79(8):777-86.
9. Tabbara KF, El-Asrar AMA, Khairallah M. Ocular infections: Infectious keratitis: Springer; 2014.
10. Khoo P, Cabrera-Aguas MP, Nguyen V, Lahra MM, Watson SL. Microbial keratitis in Sydney, Australia: risk factors, patient outcomes, and seasonal variation. Graefes Arch Clin Exp Ophthalmol. 2020;258(8):1745-55.

11. Ting DSJ, Gopal BP, Deshmukh R, Seitzman GD, Said DG, Dua HS. Diagnostic armamentarium of infectious keratitis: A comprehensive review. Ocul Surf. 2022;23:27-39.
12. Konstantopoulos A, Yadegarfar G, Fievez M, Anderson DF, Hossain P. In vivo quantification of bacterial keratitis with optical coherence tomography. Invest Ophthalmol Vis Sci. 2011;52(2):1093-7.
13. Radhakrishnan S, Rollins AM, Roth JE, Yazdanfar S, Westphal V, Bardenstein DS, et al. Real-time optical coherence tomography of the anterior segment at 1310 nm. Arch Ophthalmol. 2001;119(8):1179-85.
14. Ting DSJ, Said DG, Dua HS. Interface Haze After Descemet Stripping Automated Endothelial Keratoplasty. JAMA Ophthalmology. 2019;137(10):1201-2.
15. Darren Shu Jeng T, Sathish S, Jean-Pierre D. Epithelial ingrowth following laser in situ keratomileusis (LASIK): prevalence, risk factors, management and visual outcomes. BMJ Open Ophthalmology. 2018;3(1):e000133.
16. Almaazmi A, Said DG, Messina M, Alsaadi A, Dua HS. Mechanism of fluid leak in non-traumatic corneal perforations: An anterior segment optical coherence tomography study. Br J Ophthalmol. 2020;104(9):1304-9.
17. Li J, Ren SW, Dai LJ, Zhang B, Gu YW, Pang CJ, et al. Bacterial Keratitis Following Small Incision Lenticule Extraction. Infect Drug Resist. 2022;15:4585-93.
18. Ganesh S, Brar S, Nagesh BN. Management of infectious keratitis following uneventful small-incision lenticule extraction using a multimodal approach – A case report. Indian J Ophthalmol. 2020;68(12).
19. Geevarghese A, Wollstein G, Ishikawa H, Schuman JS. Optical Coherence Tomography and Glaucoma. Annu Rev Vis Sci. 2021;7:693-726.
20. Abbouda A, Estrada AV, Rodriguez AE, Alió JL. Anterior segment optical coherence tomography in evaluation of severe fungal keratitis infections treated by corneal crosslinking. Eur J Ophthalmol. 2014;24(3):320-4.
21. Robaei D, Carnt N, Watson S. Established and emerging ancillary techniques in management of microbial keratitis: a review. Br J Ophthalmol. 2016;100(9):1163-70.
22. Unterhuber A, Povazay B, Bizheva K, Hermann B, Sattmann H, Stingl A, et al. Advances in broad bandwidth light sources for ultrahigh resolution optical coherence tomography. Phys Med Biol. 2004;49(7):1235-46.
23. Soliman W, Fathalla AM, El-Sebaity DM, Al-Hussaini AK. Spectral domain anterior segment optical coherence tomography in microbial keratitis. Graefe's Archive for Clinical and Experimental Ophthalmology. 2013;251(2):549-53.
24. Yamazaki N, Kobayashi A, Yokogawa H, Ishibashi Y, Oikawa Y, Tokoro M, et al. In vivo imaging of radial keratoneuritis in patients with Acanthamoeba keratitis by anterior-segment optical coherence tomography. Ophthalmology. 2014;121(11):2153-8.
25. Oliveira MA, Rosa A, Soares M, Gil J, Costa E, Quadrado MJ, et al. Anterior Segment Optical Coherence Tomography in the Early Management of Microbial Keratitis: A Cross-Sectional Study. Acta Med Port. 2020;33(5):318-25.
26. Schuman JS. Spectral domain optical coherence tomography for glaucoma (an AOS thesis). Trans Am Ophthalmol Soc. 2008;106:426-58.
27. Adhi M, Liu JJ, Qavi AH, Grulkowski I, Lu CD, Mohler KJ, et al. Choroidal analysis in healthy eyes using swept-source optical coherence tomography compared to spectral domain optical coherence tomography. Am J Ophthalmol. 2014;157(6):1272-81.e1.
28. Kostanyan T, Wollstein G, Schuman JS. Evaluating glaucoma damage: emerging imaging technologies. Expert Rev Ophthalmol. 2015;10(2):183-95.
29. Donovan C, Arenas E, Ayyala RS, Margo CE, Espana EM. Fungal keratitis: Mechanisms of infection and management strategies. Survey of ophthalmology. 2021.
30. Maharana P, Sharma N, Nagpal R, Jhanji V, Das S, Vajpayee R. Recent advances in diagnosis and management of Mycotic Keratitis. Indian J Ophthalmol. 2016;64(5):346-57.
31. Cabrera-Aguas M, Khoo P, McCluskey P, Watson SL. Fungal Ocular Infections. In: Rezaei N, editor. Encyclopedia of Infection and Immunity. Oxford: Elsevier; 2022. p. 234-45.
32. Brasnu E, Bourcier T, Dupas B, Degorge S, Rodallec T, Laroche L, et al. In vivo confocal microscopy in fungal keratitis. Br J Ophthalmol. 2007;91(5):588-91.
33. Kumar RL, Cruzat A, Hamrah P. Current state of in vivo confocal microscopy in management of microbial keratitis. Semin Ophthalmol. 2010;25(5-6):166-70.
34. Kanavi MR, Javadi M, Yazdani S, Mirdehghanm S. Sensitivity and specificity of confocal scan in the diagnosis of infectious keratitis. Cornea. 2007;26(7):782-6.
35. Wang YE, Tepelus TC, Vickers LA, Baghdasaryan E, Gui W, Huang P, et al. Role of in vivo confocal microscopy in the diagnosis of infectious keratitis. Int Ophthalmol. 2019;39(12):2865-74.
36. Vaddavalli PK, Garg P, Sharma S, Sangwan VS, Rao GN, Thomas R. Role of confocal microscopy in the diagnosis of fungal and acanthamoeba keratitis. Ophthalmology. 2011;118(1):29-35.

37. Goh JWY, Harrison R, Hau S, Alexander CL, Tole DM, Avadhanam VS. Comparison of In Vivo Confocal Microscopy, PCR and Culture of Corneal Scrapes in the Diagnosis of Acanthamoeba Keratitis. Cornea. 2018;37(4).
38. Chidambaram JD, Prajna NV, Larke NL, Palepu S, Lanjewar S, Shah M, et al. Prospective Study of the Diagnostic Accuracy of the In Vivo Laser Scanning Confocal Microscope for Severe Microbial Keratitis. Ophthalmology. 2016;123(11):2285-93.
39. Villani E, Baudouin C, Efron N, Hamrah P, Kojima T, Patel SV, et al. In vivo confocal microscopy of the ocular surface: from bench to bedside. Current eye research. 2014;39(3):213-31.
40. Dart JK, Saw VP, Kilvington S. Acanthamoeba keratitis: diagnosis and treatment update 2009. Am J Ophthalmol. 2009;148(4):487-99.e2.
41. Ting DSJ, Foo VH, Yang LWY, Sia JT, Ang M, Lin H, et al. Artificial intelligence for anterior segment diseases: Emerging applications in ophthalmology. Br J Ophthalmol. 2021;105(2):158-68.
42. Zhang Z, Wang Y, Zhang H, Samusak A, Rao H, Xiao C, et al. Artificial intelligence-assisted diagnosis of ocular surface diseases. Front Cell Dev Biol. 2023;11:1133680.
43. Buisson M, Navel V, Labbe A, Watson SL, Baker JS, Murtagh P, et al. Deep learning versus ophthalmologists for screening for glaucoma on fundus examination: A systematic review and meta-analysis. Clin Exp Ophthalmol. 2021;49(9):1027-38.
44. Rampat R, Deshmukh R, Chen X, Ting DSW, Said DG, Dua HS, et al. Artificial Intelligence in Cornea, Refractive Surgery, and Cataract: Basic Principles, Clinical Applications, and Future Directions. Asia Pac J Ophthalmol (Phila). 2021;10(3):268-81.
45. Redd TK, Prajna NV, Srinivasan M, Lalitha P, Krishnan T, Rajaraman R, et al. Image-Based Differentiation of Bacterial and Fungal Keratitis Using Deep Convolutional Neural Networks. Ophthalmol Sci. 2022;2(2):100119.
46. Kuo M-T, Hsu BW-Y, Lin Y-S, Fang P-C, Yu H-J, Chen A, et al. Comparisons of deep learning algorithms for diagnosing bacterial keratitis via external eye photographs. Sci Rep. 2021;11(1):24227.
47. Wang L, Chen K, Wen H, Zheng Q, Chen Y, Pu J, et al. Feasibility assessment of infectious keratitis depicted on slit-lamp and smartphone photographs using deep learning. Int J Med Inform. 2021;155:104583.
48. Hung N, Shih AK, Lin C, Kuo M-T, Hwang Y-S, Wu W-C, et al. Using Slit-Lamp Images for Deep Learning-Based Identification of Bacterial and Fungal Keratitis: Model Development and Validation with Different Convolutional Neural Networks. Diagnostics [Internet]. 2021; 11(7).
49. Koyama A, Miyazaki D, Nakagawa Y, Ayatsuka Y, Miyake H, Ehara F, et al. Determination of probability of causative pathogen in infectious keratitis using deep learning algorithm of slit-lamp images. Sci Rep. 2021;11(1):22642.
50. Zhang Z, Wang H, Wang S, Wei Z, Zhang Y, Wang Z, et al. Deep learning-based classification of infectious keratitis on slit-lamp images. Ther Adv Chronic Dis. 2022;13:20406223221136071.
51. Kuo M-T, Hsu BW-Y, Yin Y-K, Fang P-C, Lai H-Y, Chen A, et al. A deep learning approach in diagnosing fungal keratitis based on corneal photographs. Sci Rep. 2020;10(1):14424-.
52. Kuo MT, Hsu BW, Lin YS, Fang PC, Yu HJ, Hsiao YT, et al. Deep Learning Approach in Image Diagnosis of Pseudomonas Keratitis. Diagnostics (Basel). 2022;12(12).
53. Ghosh AK, Thammasudjarit R, Jongkhajornpong P, Attia J, Thakkinstian A. Deep Learning for Discrimination Between Fungal Keratitis and Bacterial Keratitis: DeepKeratitis. Cornea. 2022;41(5):616-22.
54. Natarajan R, Matai HD, Raman S, Kumar S, Ravichandran S, Swaminathan S, et al. Advances in the diagnosis of herpes simplex stromal necrotising keratitis: A feasibility study on deep learning approach. Indian J Ophthalmol. 2022;70(9):3279-83.
55. Li J, Wang S, Hu S, Sun Y, Wang Y, Xu P, et al. Class-Aware Attention Network for infectious keratitis diagnosis using corneal photographs. Comput Biol Med. 2022;151(Pt A):106301.
56. He K, Zhang X, Ren S, Sun J, editors. Deep residual learning for image recognition. Proceedings of the IEEE conference on computer vision and pattern recognition; 2016.
57. Huang G, Liu Z, Van Der Maaten L, Weinberger KQ, editors. Densely connected convolutional networks. Proceedings of the IEEE conference on computer vision and pattern recognition; 2017.
58. Sandler M, Howard A, Zhu M, Zhmoginov A, Chen LC, editors. MobileNetV2: Inverted Residuals and Linear Bottlenecks. 2018 IEEE/CVF Conference on Computer Vision and Pattern Recognition; 2018 18-23 June 2018.
59. Simonyan K, Zisserman A. Very deep convolutional networks for large-scale image recognition. arXiv preprint arXiv:14091556. 2014.
60. Ganaie MA, Hu M, Malik AK, Tanveer M, Suganthan PN. Ensemble deep learning: A review. Engineering Applications of Artificial Intelligence. 2022;115:105151.
61. Hu S, Sun Y, Li J, Xu P, Xu M, Zhou Y, et al. Automatic Diagnosis of Infectious Keratitis Based on Slit Lamp Images Analysis. J Pers Med. 2023;13(3).
62. Wu X, Qiu Q, Liu Z, Zhao Y, Zhang B, Zhang Y, et al. Hyphae Detection in Fungal Keratitis Images With Adaptive Robust Binary Pattern. IEEE Access. 2018;6:13449-60.

63. Liu Z, Cao Y, Li Y, Xiao X, Qiu Q, Yang M, et al. Automatic diagnosis of fungal keratitis using data augmentation and image fusion with deep convolutional neural network. Comput Methods Programs Biomed. 2020;187:105019.
64. Lv J, Zhang K, Chen Q, Chen Q, Huang W, Cui L, et al. Deep learning-based automated diagnosis of fungal keratitis with in vivo confocal microscopy images. Annals of Translational Medicine. 2020;8(11):706.